Ultrasonics 64 (2016) 186–195

Contents lists available at ScienceDirect

Ultrasonics

journal homepage: www.elsevier.com/locate/ultras

Characterization of mechanical properties of materials using ultrasound broadband spectroscopy

Megha Agrawal [a], Abhinav Prasad [a], Jayesh R. Bellare [b], Ashwin A. Seshia [a,*]

[a] Nanoscience Center, Department of Engineering, University of Cambridge, CB3 0FF, UK
[b] Department of Chemical Engineering, Department of Biosciences and Bioengineering, Indian Institute of Technology, Bombay, 400076, India

ARTICLE INFO

Article history:
Received 3 February 2015
Received in revised form 8 June 2015
Accepted 2 September 2015
Available online 9 September 2015

Keywords:
Ultrasonic transducers
Material characterization
Acoustic sensor
Non-destructive testing
Resonant ultrasound spectroscopy

ABSTRACT

This article explores the characterization of homogenous materials (metals, alloys, glass and polymers) by a simple broadband ultrasonic interrogation method. The novelty lies in the use of ultrasound in a continuous way with very low input power (0 dBm or less) and analysis of the transmitted acoustic wave spectrum for material property characterization like speed of sound, density and dimensions of a material. Measurements were conducted on various thicknesses of samples immersed in liquid where continuous-wave, frequency swept ultrasonic energy was incident normal to the sample surface. The electro-acoustic transmission response is analyzed in the frequency domain with respect to a specifically constructed multi-layered analytical model. From the acoustic signature of the sample materials, material properties such as speed of sound and acoustic impedance can be calculated with experimentally derived values found to be in general agreement with the literature and with pulse-echo technique establishing the basis for a non-contact and non-destructive technique for material characterization. Further, by looking at the frequency spacing of the peaks of water when the sample is immersed, the thickness of the sample can be calculated independently from the acoustic response. This technique can prove to be an effective non-contact, non-destructive and fast material characterization technique for a wide variety of materials.

1. Introduction

Precise non-destructive quantification of the mechanical properties of solid samples (including dimensional and morphological information) is of interest for both fundamental studies to establish accurate values of material constants and in various applications involving sample identification and quantifying sample quality. Though there are many techniques available to establish dimensional and/or morphological information across various length scales, extraction of fundamental material constants (e.g. elastic moduli and density), often is relatively tedious and complex in terms of sample preparation, measurement methods and data analysis. Furthermore, many of the existing methods are not fundamentally scalable or are significantly limited by practical constraints for sample dimensions below a few millimeters.

Among the various approaches for materials characterization currently pursued, acoustic techniques provide some of the most accurate methods for extracting fundamental material constants through non-destructive means. Pulse-echo ultrasonic methods are commonly pursued to determine the speed of sound in solids, where a single short pulse of high frequency is incident normal to the surface and a time-of-flight record of the reflected ultrasonic wave from the solid is analyzed to estimate speed of sound given the distance traveled in the round trip. Various methods for velocity measurement using pulse-echo methods have been previously described in a number of reviews including Truell et al. [1]. However, pulse-echo techniques require good transducer-to-sample coupling and the signal-to-noise ratio (SNR) can be limited by inaccuracies in phase measurements, particularly in dispersive and attenuating media [2]. On the other hand, other methods based on continuous wave systems such as resonance methods and composite oscillators have also been employed [1]. Continuous wave techniques that rely on the measurement of resonance frequencies [3] (rather than signal amplitudes and/or phase) are not limited by the same practical issues outlined above for pulse-echo measurements. The resonance frequency of the lowest mode is related to the path length and the phase velocity of the continuous wave corresponding to the standing wave field [1]. Characterization of macroscopic solid or liquid samples is usually conducted using ultrasound transducers operating in the audio frequency or low

* Corresponding author. Tel.: +44 (0)1223 760333; fax: +44 (0)1223 760309.
E-mail addresses: ma547@cam.ac.uk (M. Agrawal), ap676@cam.ac.uk (A. Prasad), jb@iitb.ac.in (J.R. Bellare), aas41@cam.ac.uk (A.A. Seshia).

http://dx.doi.org/10.1016/j.ultras.2015.09.001
0041-624X/

hundreds of kHz regime [1]. Techniques such as a resonant ultrasound spectroscopy (RUS) [4] interrogate the sample at higher frequencies but are limited by constraints on extensive sample preparation and sample alignment, as well as on data analysis and interpretation.

In this paper, we propose the use of continuous wave methods at higher frequencies (several MHz) with a view toward ultimately enabling a miniaturized version of the device. Samples are characterized in a non-contact mode wherein the sample is immersed in a liquid-filled chamber and held between two high frequency broadband ultrasound transducers. The measured transmission response is then interpreted using a multi-layered transmission-matrix (T-matrix) based analytical model to obtain estimates on parameters such as the speed of sound, acoustic impedance and sample thickness. In the simplest format, this analytical model considers one-dimensional wave propagation through at each interface taking into account the material properties in the various media. An excellent agreement has been obtained for experiments conducted on thin homogenous plate samples corresponding to different materials. This paper also discusses some of the scaling considerations involved in the construction of a miniaturized portable format for this setup enabled by micro-fabrication technology with potential application to the characterization of micron-scale samples in microfluidic devices [5].

2. Theoretical model

2.1. Acoustic wave propagation – analytical basis

The simplest model for such a device is developed by considering propagation of acoustic waves through 3 layered media. In this model, two identical layers are separated by a homogenous sample medium of uniform thickness L. Acoustic plane waves are assumed to be normally incident on the layers with no reflections following the interface between the second and third media. In this analysis, we assume negligible losses at the piezoelectric–liquid interface and minimal scattering of ultrasound; viscosity in the media has also been ignored. The schematic representation of the model is shown in Fig. 1(a). The incident, reflected and transmitted waves across each interface are shown under steady-state. The incident wave has a mono-frequency carrier and by applying the continuity of normal specific acoustic impedances, the transmission coefficient can be derived [6,7].

Fig. 1 (b) shows a typical transmission response in schematic for a 3 layer system for one peak. The parameters are defined as shown in the figure. The peak frequency at the highest transmission is defined as f_{peak}. The half of the bandwidth at 50% pressure transmission coefficient is defined as Δf.

The density of the material is defined by ρ. The bulk speed of sound is defined as c (Eq. (1)), the bulk moduli is given by K and the shear moduli is given by G. The acoustic impedance of the material Z (Eq. (2)) is obtained from the density and the speed of sound in the material. k_m, also known as wave number, is a complex quantity with real part defined as the ratio of angular frequency to the speed of sound in the medium m-and imaginary part expressed by the acoustic attenuation factor α_m (Eq. (3)). For water the attenuation is taken as 25×10^{-15} Np s^2/m [6].

$$c^2 = \frac{K + 4/3G}{\rho} \tag{1}$$

$$Z = \rho * c \tag{2}$$

$$k_m = \frac{\omega}{c_m} - j\alpha_m \tag{3}$$

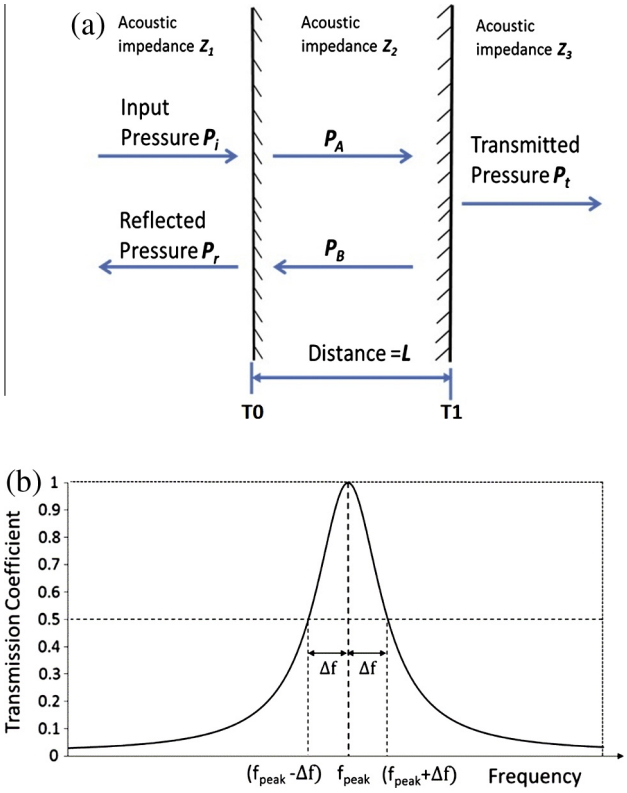

Fig. 1. (a) Schematic model for sound wave propagation in 3 layered media with boundaries as $T0$ and $T1$. (b) Typical transmission response for a 3 layer model with definition of parameters.

By applying the following boundary conditions at each interface – (i) conservation of acoustic pressure and (ii) conservation of normal component of particle velocity – on both sides of the boundary – we can solve the system of sinusoidal incident, reflected and transmitted wave equations. In this way the pressure transmission coefficient T_p can be expressed as in Eq. (4) when the 1st and 3rd media are assumed to have the same acoustic impedance Z_{ref}. Z is the acoustic impedance for the second sample media that is sandwiched between the transmitting and receiving layers [6,7].

$$T_p = \frac{2 * Z * Z_{ref}}{2 * (Z_{ref} * Z) * \cos(kL) + i(Z_{ref}^2 + Z^2) * \sin(kL)} \tag{4}$$

A MATLAB 4.3a® model can now be constructed with material property values chosen from Table 1. For example, for a PZT–Water–PZT system, with the width of water channel

Table 1
Material properties used in models.

Material	Material properties			Reference
	Density ρ (kg/m^3)	Speed of sound c (m/s)	Characteristic impedance Z (MRayl)	
Water	998	1481	1.47	[6]
Brass, Naval	8860	4430	37.3	[10–12]
Cu	8960	4660	41.61	[9–11]
Al	2700	6320	17	[6,9–12]
Perspex	1410	2730	3.85	[9,10]
Phosphor bronze	8900	3530	31.4	[12]
PZT5H	8550	4000	34.2	[11]

L = 15 cm, a plot showing the variation of transmission coefficient (magnitude and phase) as a function of frequency can be constructed as shown in Fig. 2.

Fig. 2 shows the resonant frequency peaks of water for the cavity formed by a water channel of length L between the transducers. The transmission coefficient values go to 1 whenever the standing wave criteria is met. For this particular case, the resonant frequency is calculated to be 5 kHz as seen by both the transmission and reflection curves (Fig. 2 (a) and (b)). The resonant peak can be calculated by measuring the peak to peak frequency spacing difference in the magnitude plot or by measuring the corresponding frequency difference on the phase plot. In this work, the resonant frequency is estimated from the magnitude plot.

2.2. Assumptions: modeling and analysis

For analytical modeling of the physical system, a plane wave of incident acoustic energy was assumed to be incident normally on the material and conditions of continuity of pressure and particle velocity are assumed to be valid at all boundaries. The assumptions are listed as below and the values of material properties used in the analytical models are listed in Table 1 [6–8].

(i) Homogenous materials.
(ii) No loss at boundaries.
(iii) No shear wave is generated.
(iv) Incidence angle for longitudinal wave is normal to the surface.
(v) Viscous effects can be neglected for the bulk material in static condition.
(vi) Variation of speed of sound with temperature is considered as zero.
(vii) One dimensional mono-frequency waves are incident.
(viii) No transient effects that may have existed initially are considered.

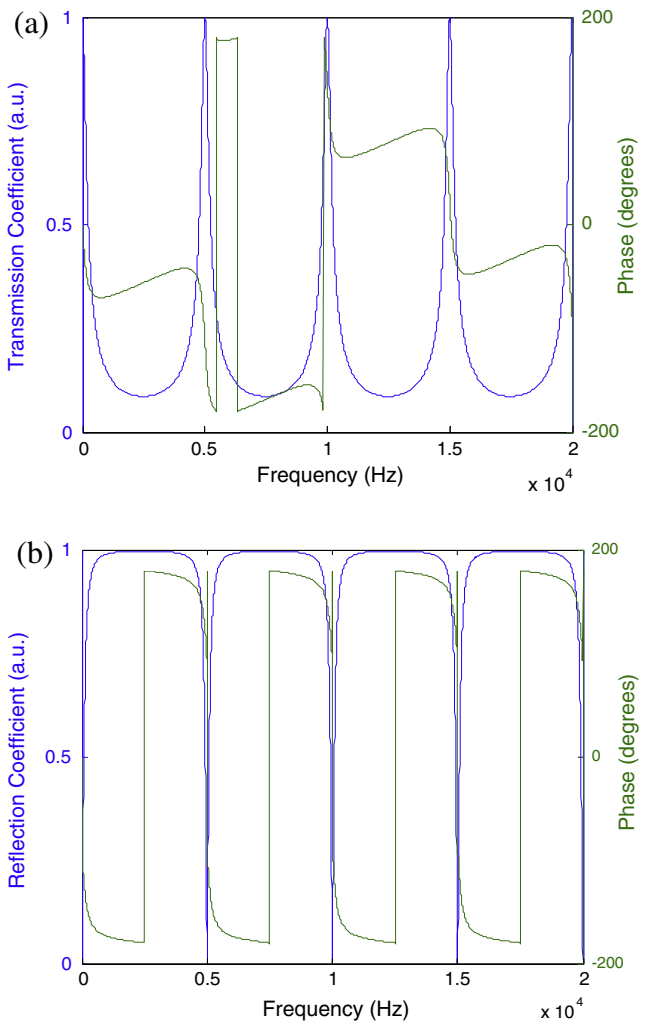

Fig. 2. Analytical model for sound wave propagation in 3 layered media (PZT–Water–PZT system) for 15 cm water channel. (a) Transmission response. (b) Reflection response. Blue is magnitude. Green is phase. (For interpretation of the references to color in this figure legend, the reader is referred to the web version of this article.)

2.3. Inverse modeling

The measured electro-acoustic frequency response for the sample provides a signature of the material properties. It is then possible to invert measured data to obtain elastic properties of the sample assuming the model above provides a sufficiently good approximation. In this section we deal with basic parameters – speed of sound and acoustic impedance of the material as described in the sections below:

2.3.1. Speed of sound

The response of the acoustic device corresponding to the model described herein will exhibit maximal response at characteristic resonance frequencies. The transmission or reflection coefficient plot with respect to frequency shows the fundamental resonance as well as higher harmonics. If the fundamental resonance frequency of nth and $(n+1)$th harmonic is given by f_n and f_{n+1} for a given sample then the resonant frequency of the sample Δf_{peak} can be given by Eq. (5) and can be related to speed of sound by the standard relation (6).

$$\Delta f_{peak} = f_{n+1} - f_n \tag{5}$$

$$C_m = 2 * L * \Delta f_{peak} \tag{6}$$

Hence, in Fig. 2(a) and (b), if the length of the channel is known, the speed of sound in the intermediate media can be calculated by measuring the resonant frequency from the electro-acoustic transmission plot using Eqs. (5) and (6).

2.3.2. Acoustic impedance

By extracting the fundamental resonance frequency and the half bandwidth value from the acoustic response the model can be employed to estimate the value of the acoustic impedance of the material to a certain degree of accuracy without *a priori* knowledge of sample dimensions. This can be seen from the Eq. (7) provided acoustic loss at these frequencies are ignored.

$$kL = \frac{\omega}{c}L = \frac{2\pi * \Delta f * L}{\Delta f_{peak} * 2 * L} = \frac{\pi * \Delta f}{\Delta f_{peak}} \tag{7}$$

By using the system-defined values for Z_{ref} – the acoustic impedance in the unknown sample can be calculated through (8) by solving the quadratic equation for unknown Z as shown by Eqs. (9) and (10). The measured quantities in Eq. (8) are f_{peak} and Δf, and $|T|$ at a particular frequency.

$$|T|^2 = \frac{4 * Z^2 * Z_{ref}^2}{\left(4 * Z_{ref}^2 * Z^2\right) * \cos^2(kx) + \left(Z_{ref}^2 + Z^2\right)^2 * \sin^2(kx)} \tag{8}$$

For example at $|T| = 0.5$, i.e. 50% transmission coefficient from the pressure magnitude transmission response, Eq. (8) can be represented as a quadratic Eqs. (9) and (10) in terms of Z^2.

$$\left(4 * Z_{ref}^2 * Z^2\right) * \cos^2(kx) + \left(Z_{ref}^2 + Z^2\right)^2 * \sin^2(kx) = 16 * Z^2 * Z_{ref}^2 \tag{9}$$

$$Ac * Z^4 + Bc * Z^2 + C = 0 \tag{10}$$

where

$$Ac = \sin^2(kx)$$
$$Bc = 4 * Z_{ref}^2 * \cos^2(kx) + 2^* Z_{ref}^2 * \sin^2(kx) - 16 * Z_{ref}^2$$
$$C = Z_{ref}^4 * \sin^2(kx)$$

$$\begin{bmatrix} A_i \\ B_r \end{bmatrix} = T_1 * T_2 * T_3 * \cdots * T_n \begin{bmatrix} T_t \\ 0 \end{bmatrix} \tag{11}$$

$$\begin{bmatrix} A_1 \\ B_1 \end{bmatrix} = \underbrace{\frac{1}{2z_2}\begin{bmatrix} (z_1+z_2)e^{-i(k_2-k_1)x_1} & (z_2-z_1)e^{i(k_2+k_1)x_1} \\ (z_2-z_1)e^{-i(k_2+k_1)x_1} & (z_2+z_1)e^{i(k_2-k_1)x_1} \end{bmatrix}}_{T \text{ matrix at boundary } 1=T_1} \begin{bmatrix} A_2 \\ B_2 \end{bmatrix} \tag{12}$$

$$\begin{bmatrix} A_2 \\ B_2 \end{bmatrix} = \underbrace{\frac{1}{2z_3}\begin{bmatrix} (z_2+z_3)e^{-i(k_3-k_2)x_2} & (z_3-z_2)e^{i(k_3+k_2)x_2} \\ (z_3-z_2)e^{-i(k_3+k_2)x_2} & (z_3+z_2)e^{i(k_3-k_2)x_2} \end{bmatrix}}_{T \text{ matrix at boundary } 1=T_2} \begin{bmatrix} A_3 \\ B_3 \end{bmatrix} \tag{13}$$

The transmission and reflection response for a 3-layer system is calculated and represented by Eqs. (14) and (15) respectively by solving Eqs. (11)–(13) analytically.

$$T = \frac{4z_2z_3}{(z_1+z_2)(z_2+z_3)(z_3+z_4)e^{-i(k_2x_1-k_1x_1+k_3x_2-k_2x_2+k_4x_3-k_3x_3)} + (z_3-z_2)(z_2-z_1)(z_3+z_4)e^{i(k_2x_1+k_1x_1-k_3x_2-k_2x_2)}} \tag{14}$$

$$R = \frac{z_2(z_2+z_3)(z_2-z_1)e^{-i(k_2x_1+k_1x_1+k_3x_2-k_2x_2)} + (z_2+z_1)(z_3+z_2)e^{i(k_2x_1-k_1x_1-k_3x_2-k_2x_2)}z_3}{(z_1+z_2)(z_2+z_3)(z_3+z_4)e^{-i(k_2x_1-k_1x_1+k_3x_2-k_2x_2+k_4x_3-k_3x_3)} + (z_3-z_2)(z_2-z_1)(z_3+z_4)e^{i(k_2x_1+k_1x_1-k_3x_2-k_2x_2)}} \tag{15}$$

2.4. T-matrix model – for more than 3 layers

When there are more than 3 layers of different media, the T-matrix formulation can be extended to describe the response observed. The schematic for a multiple layer system with acoustic wave propagation is as shown in Fig. 3. The total acoustic transmission response can be summarized and represented in the form of the Eq. (11) where the transmission coefficient at the last layer would be the multiplication of transmission coefficients at each boundary, as shown by Eqs. (12) and (13). A_i and B_r are the incident acoustic wave and the reflected acoustic wave on the first boundary respectively. $T_1, T_2, \ldots, T_n$ are the individual transmission coefficients matrix at each boundary n. T_t is the total transmitted acoustic wave at the last medium. Since the last medium is assumed to be on infinite length, there is no reflected acoustic wave in that medium, indicated by the 0 in the matrix.

The 4 layer, 5 media system was thereafter modeled in MATLAB 4.3a®, considering PZT–Water–Sample–Water–PZT layers. The magnitude of the pressure transmission coefficient for the T-matrix system for a Copper sample is as shown in Fig. 4. The water channel on each side was 7.4 mm long and the thickness of the Cu sample was taken to be 2 mm. From Fig. 4(c), it is seen that the peak spacing is approximately 10 kHz, corresponding to the expected response for water. The final response is a superposition of the various resonant modes with the relative maxima and minima obtained due to the interference of the overlapping modes [13]. To illustrate this and to separate the effect of individual peaks of different materials, the transmission response is plotted by dividing the system into two 3 layer models each as shown in Fig. 4(b) and (c). The response for the PZT–Water–Copper–Water–PZT, 5 layer model is as shown in Fig. 4(a). The individual response of just the 2 mm thick Copper plate is as shown in

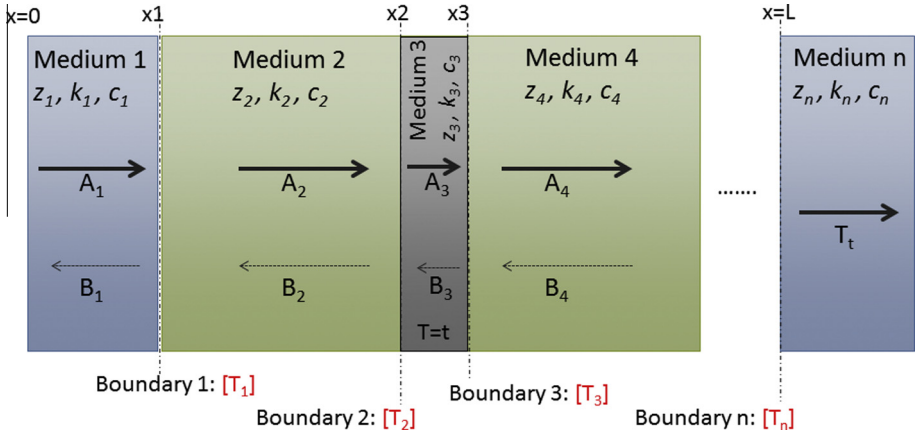

Fig. 3. Schematic for the T-matrix model for n materials with parameter definition. Z_n represents acoustic impedance, k_n represents wave number, c_n is the speed of sound in the medium. L represents the length of the water channel. $T = t$ represents the thickness of the sample (also $x3$–$x2$, here). ***A*** represents incident wave, ***B*** represents the reflected wave in each media, $\boldsymbol{T_t}$ represents the transmitted wave in the last medium.

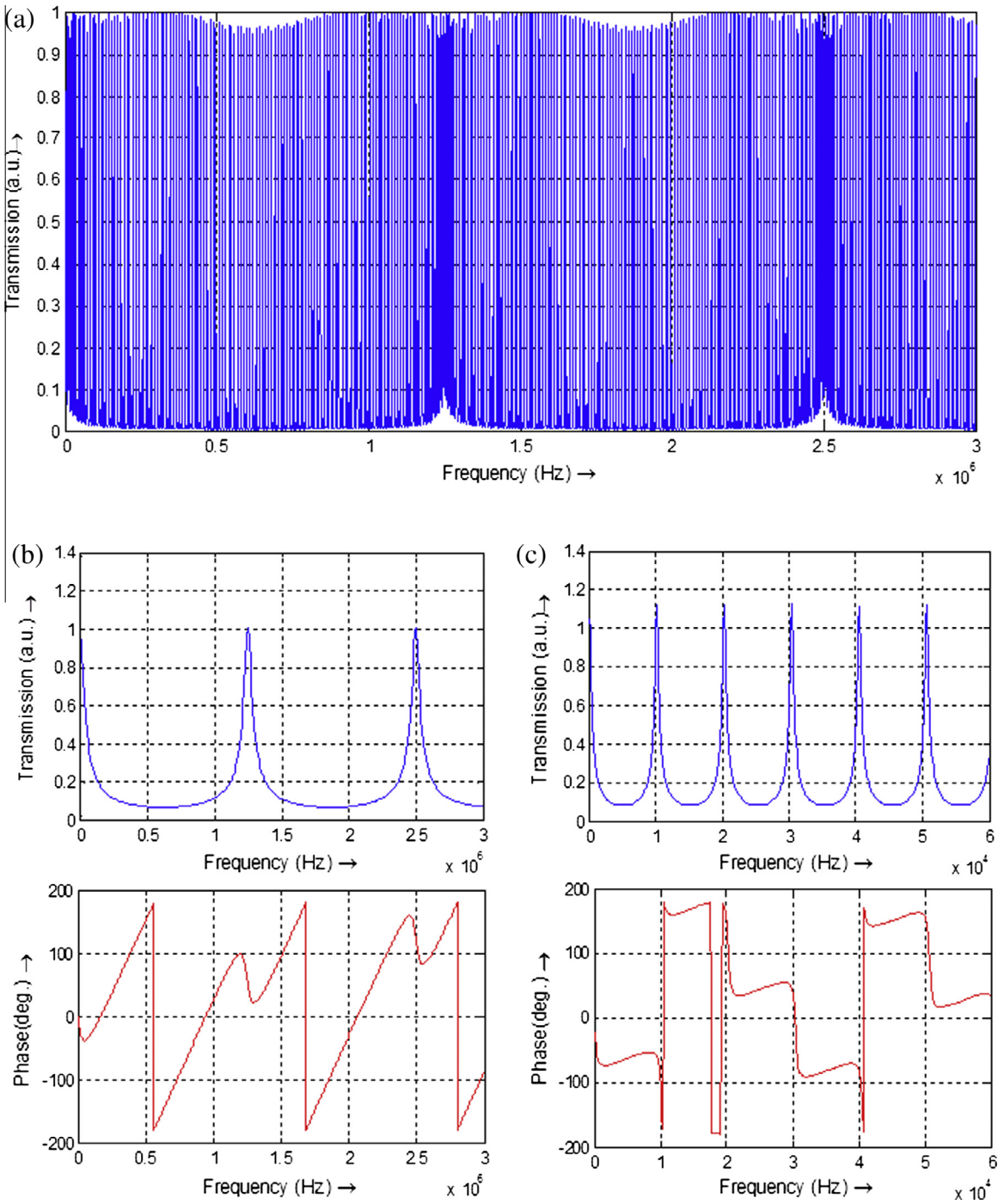

Fig. 4. (a) Analytical model for sound wave propagation in 5 layered media with PZT–Water–Cu–Water–PZT. (Thickness 2 mm). (b) Analytical model for 3 layer Water–Cu–Water. (c) Analytical model for 3 layer PZT–Water–Cu.

Fig. 4(b) modeled by Water–Cu–Water 3 layered model. It can be seen that the peak separation follows the speed of sound in Copper as calculated by Eq. (6). The response for PZT–Water–Cu system is as shown in Fig. 4(c), which would be similar for the Cu–Water–PZT case on the other side of the sample Cu plate by symmetry.

2.4.1. Thickness measurement

If the metal sample of thickness t, is placed at the midpoint of the length of the water channel D, then the distance $x1$ between the boundary of PZT–Water and Water Metal is equal to $(D-t)/2$. Similarly the distance $x4$ between the boundary between Metal–Water and Water–PZT is also $(D-t)/2$. The speed of sound of water $C_w = 1500$ m/s. $D = 0.15$ m.

From the acoustic response, the difference in frequency between alternative peaks of water can be measured, *delF*. The thickness of the sample, when the sample is placed at the midpoint in the water channel can be defined as

$$\frac{(D-t)}{2} = \frac{C_w}{2 * delF} \tag{16}$$

The resolution of thickness detection can be improved by increasing the total number of data points in the given frequency span when studying the zoomed in peaks corresponding to water in the measured response.

2.5. Scaling analysis

An important aspect of the proposed device is the potential scalability to a micro-fabricated format to enable the characterization of microscopic samples and biological specimens in fluidic environments [5]. To examine the impact of geometrical scaling of the device on system resolution two cases are considered:

(i) Decreasing sample dimensions.
(ii) Increasing operating frequencies.

The analytical model presented in this paper can be utilized to examine the impact of dimensional scaling. It is observed that as the length of the sample decreases, as seen from Eq. (6) and as reported in [5], the separation between the resonant peaks increases and hence the ability to resolve the spacing between the peaks to calculate the speed of sound is enhanced assuming all other parameters remain scale invariant. A theoretical analysis for Copper plates of four different thicknesses used in our experiments is shown in Fig. 5, where the peak-to-peak distance between the different sample thicknesses increases by the same factor by which the length decreases. The same is later verified by experiments shown in Fig. 8. This justifies the motivation for using microfabricated platforms to enable characterization of miniaturized samples. Analytically, the limit of dimensional resolution (L_r), which determines the least resolvable dimension of the sample, depends directly on the speed of sound in the material i.e. on stiffness and density of the material, and inversely on the frequency bandwidth of transducers and is given by Eq. (17).

$$L_r = \frac{c}{2f_{BW}} \tag{17}$$

Further, a second limit on the dimensional resolution is governed by the wave diffraction limit set by the order of the wavelength of the acoustic wave and can also be approximately calculated from Eq. (17) by replacing f_{BW} by the center frequency of the transducer. In the experimental set-up presented in this work, the center frequency and frequency bandwidth were both

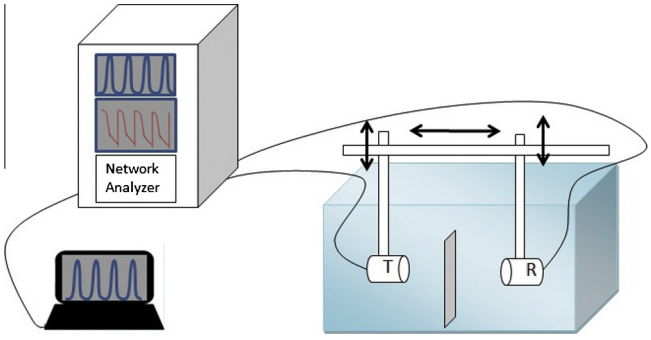

Fig. 6. Experimental setup block diagram.

10 MHz which would imply a limit of resolution of approximately 230 μm for Copper samples and a higher resolution in materials where the speed of sound is lower.

By simultaneously increasing the operating frequency, the frequency bandwidth proportionately increases, and hence the limit on dimensional resolution can be improved even further. As the center frequency for piezoelectric transducers depends inversely on the material thickness, a piezoelectric elements fabricated by thin-film MEMS processing can provide transducers operating in the 1 GHz range [14]. Increased frequency bandwidth can also improve the frequency range over which a larger number of samples could be analyzed. Further, sample measurements could also be carried out using higher harmonics with increased peak-to-peak spacing enabling improved frequency resolution or sample discrimination for cases of two different materials whose values for speed of sound are comparable as shown by the present authors [5].

Another calculation to support this design specification [14] is that for resonator models to have sufficient reflections in the resonant cavity the requirement is $\alpha_{xL} < 1$. For micron sized channels assuming a path length for the channel is $xL = 100$ μm, then an approximate limit for such measurements is $\alpha < 10{,}000\ \mathrm{m}^{-1}$. For water based samples the acoustic attenuation α, has values $\alpha/f^2 \approx 25 \times 10^{-15}\ \mathrm{m}^{-1}\ \mathrm{s}^2$. This corresponds to an upper frequency limit of 632.455 MHz.

Hence, this scaling analysis shows that system miniaturization enabled by microfabrication and embedded miniaturized high-frequency transducers provides an opportunity to improve system resolution.

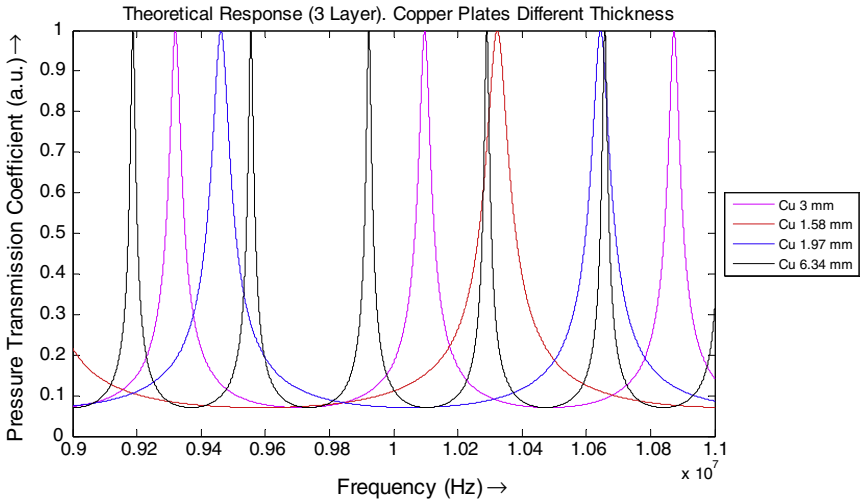

Fig. 5. Analytical acoustic response for different thickness of copper plates in water showing an increasing frequency spacing for plates of smaller thickness.

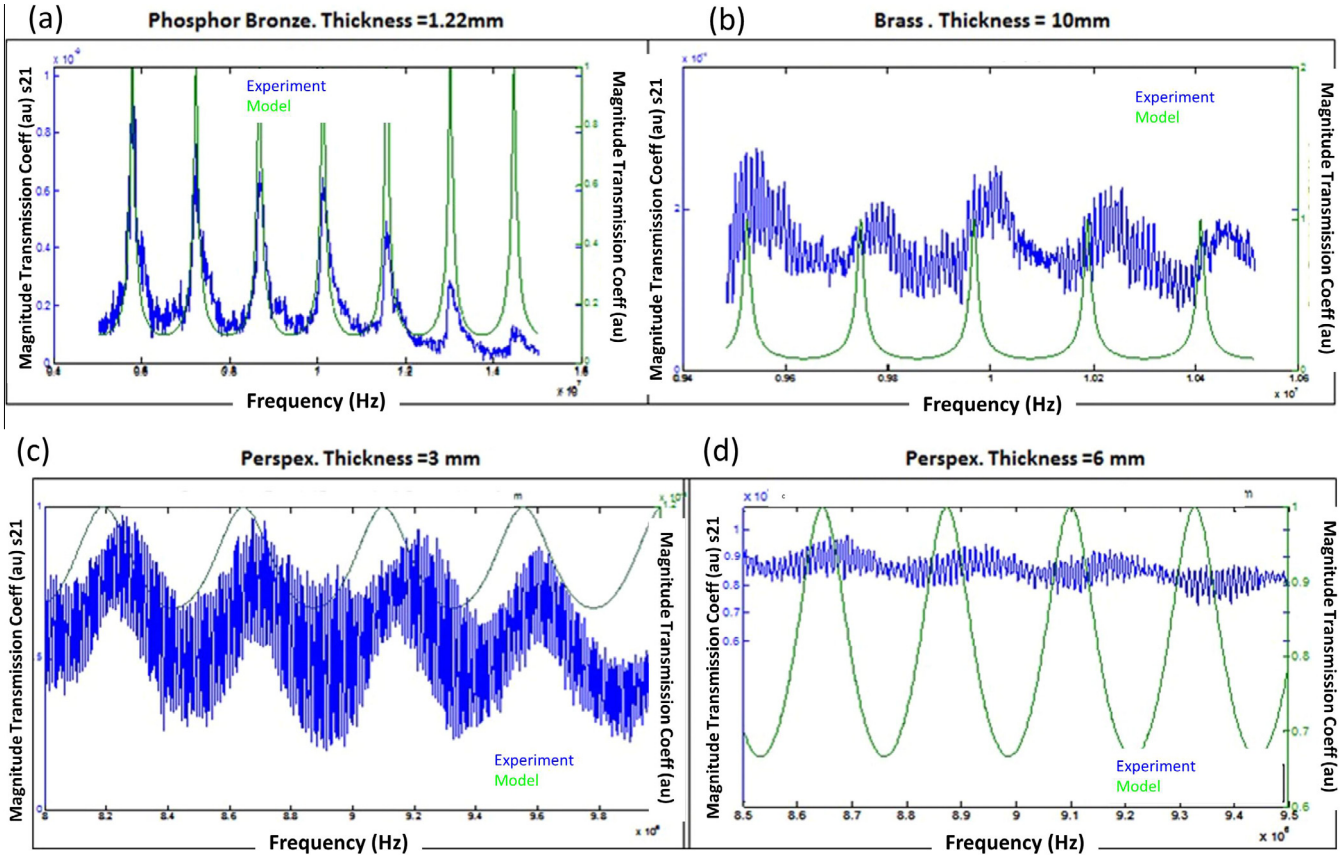

Fig. 7. Experimental results and theoretical model plots for various materials: (a) phosphor bronze (1.22 mm), (b) brass (10 mm), (c) perspex (3 mm), and (d) perspex (6 mm).

3. Experimental methods

3.1. Setup

As shown schematically in Fig. 6, the experimental setup consists of a water tank filled with degassed DI water at room temperature (23.2 °C). Two immersion type water matched single-element ultrasonic transducers (focused type, 10 MHz, Olympus, USA) suspended with adjustable frames and connected to a Network Analyzer were used. One transducer (labeled T) acted as the transmitter and was connected to the output port of the network analyzer that supplied a swept frequency, constant amplitude signal (−3 dBm) signal to the transmitter. The other transducer *R* acted as the receiver and was connected to the input port of the network analyzer. The transmission (S21) parameter was recorded on a computer for further analysis.

3.2. Working principle

Broadband water-matched ultrasonic transducers with a center frequency of 10 MHz and bandwidth of 8–10 MHz were employed (response shown in the Appendix A) with an approximately flat or constant (same amplitude) response over the swept frequency range. The distance between the transducers were fixed at 15 cm as the focus of each transducer was at around 7.5 cm. Plate samples of different materials with varying thicknesses were placed in the path of insonication and at approximately the mid-point of the distance between the transducers. The used samples, procured from RS-online [9], are listed along with the results in Table 2.

3.3. Traditional pulse-echo technique comparison

The set of samples used in the broadband water-matched ultrasonic transducers experiment were also measured to determine the speed of sound using the traditional approach by using pulse-echo ultrasonic technique. A 5 MHz Sonatest SLE 5-10 507/7 ultrasonic transducer probe was used for this purpose. Balteau Sonatest Sitescan 100 was used to excite the transducer as well as to receive the ultrasonic pulse. To calibrate the system Sonatest Universal Test block made of stainless steel (speed of sound 5930 m/s, thickness 20 mm) was used. The probe was put on the surface of the calibration block with the help of a lubricant and a characteristic amplitude-time response was obtained on the pulser receiver system oscilloscope. The observed peaks of the received ultrasonic pulse were observed on the oscilloscope at every 20% of the time scale, hence the calibration of the time scale was calculated to be $2t = \frac{(2\times 20\times 10^{-3})}{5930}$; $t = 3.372$ μs.

After calibration, pulse-echo tests were performed on all the samples. The time difference between consecutive peaks were observed on the oscilloscope, the thickness of the sample was measured using the vernier calipers (Mitutoyo Absolute Digimatic, Japan) and the speed of sound was calculated using the standard relationship for pulse-echo wave round trip. The results are as summarized in Table 2.

The least measurable time in the setup was $0.2 \times 3.372 \times 10^{-6}$ s and as most solid samples have their speed of sound values in the range 5000 m/s, the least resolvable thickness in the current pulse-echo method was approximately 1.5 mm.

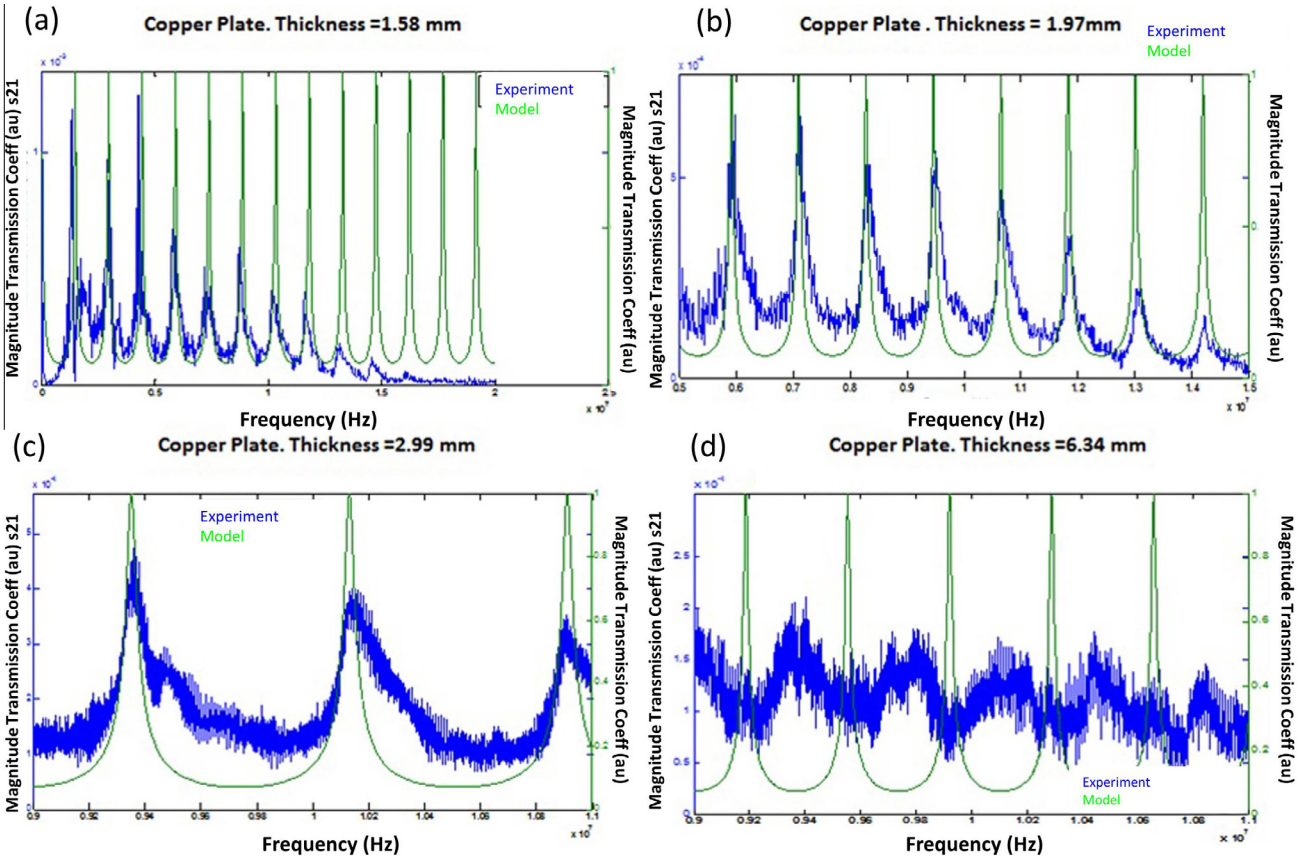

Fig. 8. Transmission response plots showing comparison between theory and experiment for various thicknesses of copper plates. (a) 1.58 mm, (b) 1.97 mm, (c) 2.99 mm, and (d) 6.34 mm.

Table 2
Summary of speed of sound and thickness measurements for various materials.

Material	Thickness measured by vernier callipers (mm)	Literature speed of sound (m/s)	Measured speed of sound		Speed of sound through pulse-echo technique (m/s)	Mean speed of sound % agreement with pulse echo (%)
			Mean (m/s)	SD (m/s)		
Al	1.42	6320	6400.2	442.4	–	–
	3	6320	6555.4	423.6	6209.7	−5.56
Stainless steel	1.5	5790	6072.8	225.2	5502.6	−10.36
Brass, Naval	0.67	4430	4371.8	289.0	4358.5	−3.05
Brass	9.75	4700	4628.6	471.4	4780.7	3.18
Acrylic (Perspex)	3	2730	2720.0	4.6	2690.0	−1.11
	6	2730	2910.0	254.6	2690.0	−8.17
Copper	0.9	4660	4570.2	264.7	–	–
	1.58	4660	4601.0	233.7	–	1.93
	1.97	4660	4665.0	90.2	4251.9	−9.71
	2.99	4660	4629.1	105.7	4440.2	−4.25
	6.34	4660	4686.6	571.0	4691.6	0.11
Phosphor bronze	1.22	3530	3531.9	81.8	3843.4	8.10

4. Results and discussion

This analytical model predicts the transmission response for swept frequency ultrasound input for a particular sample of a particular dimension. This response is a signature of the sample and can be used to extract the corresponding value of speed of sound as verified by the analytical model and experiments. The analytical transmission response for the 3 layer model (Water–Sample–Water) and 5 layer model (PZT–Water–Sample–Water–PZT) along with the experimental results obtained were plotted for all the samples and a good agreement between the positions of the peak frequencies was observed. For the purpose of calculation of the speed of sound of the sample only the frequency difference between the adjacent peaks corresponding to the sample is sufficient. The peaks in the transmission response are clearly more pronounced if the acoustic impedance of the sample is much higher than that of water. The peaks of water formed in the two water chambers on the front and back of the sample interfere constructively and destructively with the response. The 3-layer theoretical model is found to be sufficient to predict the speed of sound in the media. Fig. 7 shows the transmission response for alloys – Phosphor bronze and Brass and two different thickness of the polymer Acrylic Perspex. It is observed that the peak positions and number of peaks in every particular frequency sweep range as predicted by

the model show a good match with the experiment. From the observed experimental response the speed of sound is calculated from the peak-to-peak frequency spacing using a peak detection algorithm written on MATLAB 4.3a®. The mean and standard deviation of the speed of sound was calculated for a minimum of three repeat experimental readings. The results for the calculated speed of sound for various samples are compiled and tabulated in Table 2 and compared with the values obtained from literature. The match between the values of speed of sound in literature and those obtained experimentally using this method fall within 2% error for most of the samples investigated except for Acrylic Perspex where the difference was 6.6%. As can be seen for the case of Acrylic Perspex, the specific resonant peaks are less pronounced due to the relatively close impedance matching with water which directly influences the maximum and minimum amplitude difference in the magnitude transmission coefficient response.

Fig. 8 shows the experimental and theoretical acoustic response of different thickness copper plates of the same grade. We observe that for thicker plates the theoretical and experimental peaks are not exactly matched in frequency, although the peak frequency difference and the number of peaks in this range are the same. This is potentially due to the influence of the two water channels in the front and back of the sample. Since the corresponding effective length of the water channel for these cases is decreased by a larger amount, the resonant frequency of the water is higher and hence the interference patterns are more pronounced in the final output.

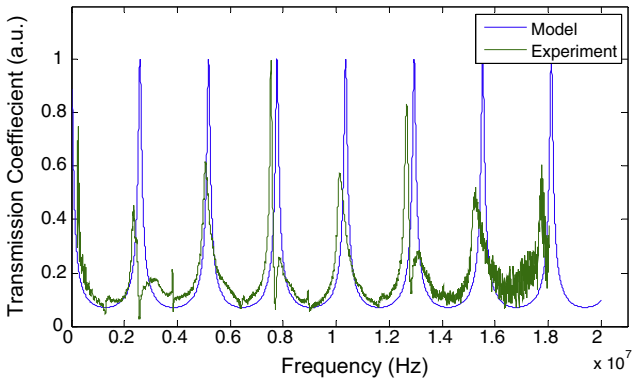

Fig. 9. Acoustic transmission response *wrt* frequency for a 0.9 mm Copper plate in water. Blue is the analytical model. Green is the experimental response normalized with the transducers' response and the maximum experimental amplitude. (For interpretation of the references to color in this figure legend, the reader is referred to the web version of this article.)

4.1. Speed of sound and thickness – By inverse calculation

The speed of sound in various materials is calculated from the experimental transmission response by inverse calculation (using Eq. (6)) after applying a peak detection algorithm. The mean and standard deviation is reported in Table 2 for different materials. For the same materials, pulse echo technique was applied as described in Section 3.3 and speed of sound was detected. The pulse-echo technique was limited to samples of thickness more than 1.5 mm because of limit of the instrumentation. The % agreement of speed of sound between ultrasound broadband technique and pulse-echo was within 10%.

4.2. Acoustic impedance using inverse calculation

The acoustic impedance of the material can be estimated from the measured transmission response as previously discussed. The procedure involves applying normalization techniques to the recorded experimental response due to the non-linear, non-flat behavior of the transducer. The experimental transmission response of the sample is first converted to a ratio by dividing through by the response of the transducers in water (i.e. without the sample present). Next, the response is normalized between values 0 to 1 by dividing with the maxima of the experimental amplitude. This technique, although approximate, provides a relatively simple yet accurate estimate of the transmission response to estimate the acoustic impedance. The normalized response in experiment is matched to that predicted by the 3-layer model for 0.9 mm Copper plate (as an example) is shown in Fig. 9. As seen the response matches closely for most of the harmonic peaks. Since the transducer is not perfectly broadband and flat not all harmonics match in amplitude. For the inverse calculation of the acoustic impedance, any point on the magnitude response can be chosen for magnitude of the transmission coefficient and the corresponding half bandwidth can be estimated to obtain the acoustic impedance. It should be noted that the calculation of acoustic impedance can be done without any information on the sample thickness, as the thickness term cancels out. Table 3 summarizes the obtained acoustic impedance of the samples at various harmonics.

Table 3
Summary of acoustic impedance measurements for various materials.

Material	Dimension (mm)	Harmonic	f_{Peak} (MHz)	*BW* at Tmag (kHz)	Tmag	*Z* (MRayl)	% Error (%)
Cu	0.25	1st	9.32	325	0.561	39.786	3.10
Cu	0.9	2nd	2.5889	120k	0.356	53.401	29.90
	0.9	2nd		200	0.250	47.507	15.58
Cu	1.58	2nd	1.4747	162k	0.356	39.733	4.51
		2nd		147	0.203	46.601	−11.99
		4th		78	0.306	55.341	−32.99
Cu	1.97	2nd	1.1827	238	0.119	41.500	0.97
	1.97	4th		66	0.379	41.100	0
Brass	0.67	2nd	3.306	185	0.439	34.486	7.54
Al	1.97	2nd	2.534	330	0.356	19.523	−14.84
Al	1.42	2nd	1.6408	360	0.328	13.466	20.79
Al	3	6th	1.0533	108	0.389	22.072	−29.83
Stainless steel	1.5	1st	1.93	78	0.442	47.232	−3.35
	1.5	2nd	1.93	122	0.321	44.017	3.68
	1.5	3rd	1.93	94	0.365	49.199	−7.66
	1.5	5th	1.93	82	0.346	60.001	−31.293
Perspex	3	2nd	0.455	108	0.886	2.988	22.40
	3	4th	0.455	166	0.703	3.833	0.45
	3	9th	0.455	118	0.780	3.810	1.03

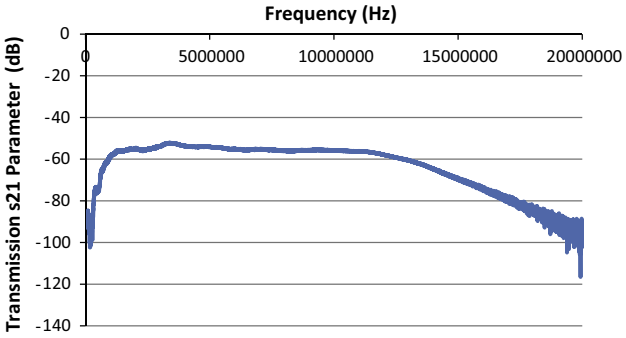

Fig. A. Transducers transmission response in water. Input power = −3 dBm.

5. Conclusions and outlook

We propose a simple, real-time, non-contact and non-destructive approach to characterize homogenous, isotropic materials and to predict the speed of sound and acoustic impedance in the material. There is a high degree of qualitative agreement between the theoretical models and experimental results for the various samples used. Quantitatively, the extracted values of speed of sound are very close to those reported in literature and are within a range of 1% for most of the tested materials. The acoustic impedance is also calculated from the measured response by adopting normalization techniques to account for the non-linear and non-flat response of the transducers and other non-idealities in the measurement process.

Although literature reports on the inherent limitations of liquid coupling methods including the operating frequency limitation imposed by the attenuation within the liquid itself [1], this limitation has been overcome in the work presented herein by using water-matched coupled transducers operating at >10 MHz enabling improved dimensional resolution in non-contact mode.

The models used here are simplified for the homogenous, isotropic case without considering losses, a more elaborate model can be constructed by considering the values of frequency-dependent attenuation behavior for various materials, from which a comprehensive library of the exact prediction for acoustic transmission could eventually be constructed and a variety of materials can be characterized.

Moreover, as supported by the scaling analysis presented here, a micro-fabricated version of the device could potentially be realized which could improve both the system resolution and the measurement bandwidth, thus, enabling analysis of a variety of miniaturized samples and providing the conceptual basis for the development of a new non-contact material characterization tool at micron scale.

Conflicts of interest

The authors declare no conflict of interest.

Acknowledgments

Funding from the BBSRC and Cambridge Trusts is gratefully acknowledged. Megha Agrawal would also like to acknowledge the fruitful discussions with her lab colleague – Ying Zhou.

Appendix A

See Fig. A.

Appendix B. Supplementary material

Supplementary data associated with this article can be found, in the online version, at http://dx.doi.org/10.1016/j.ultras.2015.09.001.

References

[1] R. Truell, C. Elbaum, B.B. Chick, Noninvasive determination of sound speeds in liquids, Ultrasonic Methods in Solid State Physics, Academic Press, New York and London, USA and UK, 1969.
[2] Y. Levy, Y. Agnon, H. Azhari, Measurement of speed of sound dispersion in soft tissues using a double frequency continuous wave method, Ultrasound Med. Biol. 32 (7) (2006).
[3] D.N. Sinha, G. Kaduchak, in: R. Celotta, T. Lucatorto (Eds.), Modern Acoustical Techniques for the Measurement of Mechanical Properties, vol. 39, first ed., Academic Press, San Diego, CA, USA, 2001 (Chapter 8).
[4] J. Maynard, Resonant ultrasound spectroscopy, Phys. Today 49 (1) (1996) 26–31, http://dx.doi.org/10.1063/1.881483.
[5] M. Agrawal, Y. Zhou, J.R. Bellare, A.A. Seshia, Design and modeling of an integrated device for acoustic resonance spectroscopy. Paper presented at the IEEE International Ultrasonics Symposium, IUS, 22–25 July 2013, pp. 2183–2186.
[6] L.E. Kinsler, A.R. Frey, A.B. Coppens, J.V. Sander, Fundamentals of Acoustics, 4th ed., John Wiley and Sons Inc., New York, NY, USA, 2000.
[7] S. Temkin, Elements of Acoustics, John Wiley and Sons Inc., New York, NY, USA, 1981.
[8] L.M. Brekhovskikh, in: R.T. Beyer (Ed.), Waves in Layered Media, Academic Press, London, UK, 1960.
[9] RS-online. <http://uk.rs-online.com/web/c/abrasives-engineering-materials/> (accessed on 01.07.14).
[10] Olympus material sound velocities. <http://www.olympus-ims.com/en/ndt-tutorials/thickness-gage/appendices-velocities/> (accessed on 01.07.14).
[11] NDT online material properties. <https://www.nde-ed.org/EducationResources/CommunityCollege/Ultrasonics/Reference%20Information/matproperties.htm> (accessed on 01.07.14).
[12] Matweb material property data. <http://www.matweb.com/> (accessed on 01.07.14).
[13] G. Guidarelli, A. Marini, L. Palmieri, Experimental method for investigating the acoustic transmissivity of fluid-loaded elastic plates, Acoust. Lett. 15 (1) (1991) 1–7.
[14] A. Jakob, M. Bender, T. Knoll, R. Lemor, T. Lehnert, M. Koch, M. Veith, et al., Comparison of different piezoelectric materials for GHz acoustic microscopy transducers. In: IEEE International Ultrasonics Symposium, pp. 1722–1725, 2009, http://dx.doi.org/10.1109/ULTSYM.2009.5442024.